Injury 57 (2026) 113043

Contents lists available at ScienceDirect

Injury

journal homepage: www.elsevier.com/locate/injury

Ischemic skin flap viability: *in vivo* study of alginate-ZIF-8 hydrogel systems with *Rhizophora mangle* and tannic acid

Bianca Rocha da Silva Barreto [a], Eduardo Carvalho Lira [b], Severino Alves Júnior [c], Luzia Abilio da Silva [b], Yuri José de Albuquerque Silva [c], Widarlane Ângela da Silva Alves [b], Madson Manoel Nunes da Silva [b], Rosallyne Hosana Vanderlei das Chagas [d], Larissa Cardeal da Rocha Carvalho [d], Jasmine Martins Vieira Cunha [d], Jamily Isabel Viana de Lima [d], Ester Francisca Gomes de Lima [d], Ícaro Mota Oliveira [e], Jeymesson Raphael Cardoso Vieira [a,*]

[a] *Department of Histology and Embryology, Biosciences Center, UFPE, Av. Professor Moraes Rego, 1235 – Cidade Universitária, 50760-420. Recife, Pernambuco, Brazil*
[b] *Department of Physiology and Pharmacology, Biosciences Center, UFPE, Av. Professor Moraes Rego – Cidade Universitária, 50670-420. Recife, Pernambuco, Brazil*
[c] *Department of Fundamental Chemistry, Exact and Natural Sciences Center, UFPE, Av. Professor Luiz Freire – Cidade Universitária, 50740-540. Recife, Pernambuco, Brazil*
[d] *Biosciences Center, UFPE, Av. Professor Moraes Rego, 1235 – Cidade Universitária, 50760-420. Recife, Pernambuco, Brazil*
[e] *São Carlos Chemistry Institute, USP, Av. Trabalhador Sancarlense – Parque Arnold Shcimidt, 13566-590. São Carlos, São Paulo, Brazil*

ARTICLE INFO

Keywords:
Biocompatible materials
Pedicled flaps
Rhizophora mangle
Tannins
Metal-organic frameworks
Alginates
Hydrogels

ABSTRACT

Skin flaps are widely used in plastic and reconstructive surgery. However, inadequate blood perfusion during flap mobilization can trigger an ischemic process that may lead to tissue necrosis in the absence of effective management of the inflammatory process. In this context, the search for new biocompatible strategies to ensure the viability of ischemic skin flaps (ISFs) remains necessary. Therefore, this study evaluated novel alginate-ZIF-8 (ALG-ZIF-8) hydrogel systems with *Rhizophora mangle* (*R. mangle*) extract and tannic acid (TA) to assess their potential in preventing necrosis in ISF. Twenty-two male Wistar rats underwent the surgical creation of ISF and were divided into four groups: 0.9% saline (negative control - NegC), placebo alginate hydrogel (pALGgel), ALG-ZIF-8 hydrogel system with 5% TA (ALGzTA), and finally, ALG-ZIF-8 hydrogel system with 5% *R. mangle* (ALGzRm). Flap outcomes were evaluated through macroscopic observation, followed by morphometric analysis of viable and necrotic areas, and histomorphometric analysis of fibroblasts, blood vessels, and leukocytes, using ImageJ and PrimeCam 5.1 software. Statistical analysis was performed using IBM SPSS software (version 27). The results suggest that the formulations produced divergent outcomes by differentially modulating inflammatory and angiogenic responses. The ALGzRm formulation tended to show a protective profile, associated with a significant reduction in leukocyte infiltration ($p < 0.001$), while the ALGzTA formulation was linked to a detrimental response, including exacerbated inflammation and a pathologically high blood vessel count ($p = 0.015$). In conclusion, findings suggest that the ALGzRm-gel has a potential for tissue repair, mediated by the modulation of inflammatory and angiogenic responses.

Introduction

The skin is the largest organ of the human body by weight and surface area [1,2], composed primarily of the epidermis, an outer epithelial layer, and the dermis, a deep layer consisting mainly of connective tissue [3]. Below the dermis lies the hypodermis, a subcutaneous

* Corresponding author at: Department of Histology and Embryology, Biosciences Center, UFPE, *Av.* Professor Moraes Rego, 1235 – Cidade Universitária, 50760-420. Recife, Pernambuco, Brazil.

E-mail addresses: bianca.barreto@ufpe.br (B.R.S. Barreto), eduardo.carvalholira@ufpe.br (E.C. Lira), severino.alvesjr@ufpe.br (S.A. Júnior), luzia.abilio@ufpe.br (L.A. da Silva), yuri.albuquerque@ufpe.br (Y.J.A. Silva), widarlane.angela@ufpe.br (W.Â.S. Alves), madson.silva@ufpe.br (M.M.N. da Silva), rosallyne.chagas@ufpe.br (R.H.V. Chagas), larissa.cardeal@ufpe.br (L.C.R. Carvalho), jasmine.martins@ufpe.br (J.M.V. Cunha), jamily.isabel@ufpe.br (J.I.V. de Lima), ester.francisca@ufpe.br (E.F.G. de Lima), icaro.mio@hotmail.com (Í.M. Oliveira), jeymesson.vieira@ufpe.br (J.R.C. Vieira).

https://doi.org/10.1016/j.injury.2026.113043
Accepted 26 December 2025
Available online 10 January 2026

tissue composed mostly of adipose tissue pads [4]. Skin flaps (or cutaneous flaps) are skin segments transferred from a donor site to a recipient site, maintaining their necessary blood supply through a pedicle to ensure the flap's survival [5,6]. This procedure is frequently used in plastic and reconstructive surgery [7,8]. However, complications can occur during the transfer of these flaps, notably a lack of blood perfusion and subsequent ischemia, which characterizes an ischemic skin flap (ISF). The failure to effectively manage this inflammatory process can result in tissue necrosis [8,9]. Therefore, maintaining blood supply is an essential factor for ensuring the viability and survival of ISFs [5]. To address the challenge of ISF necrosis, various therapeutic strategies have been explored to enhance flap viability. These include pharmacological interventions such as vasodilators (*e.g.*, nitroglycerin) to improve perfusion [68,69], anticoagulants to prevent microthrombosis [70], and antioxidants or reactive oxygen species (ROS) scavengers to counteract ischemia-reperfusion injury [71]. Additionally, approaches aimed at promoting angiogenesis, including cell-based therapies and modulation of pathways involving nitric oxide (NO), have been investigated [72]. Despite extensive existing research, new biocompatible approaches are still needed [5,10].

In response to this demand, the use of biomaterials has emerged as a promising alternative, defined as engineered substances designed to interact with living systems to direct therapeutic or diagnostic procedures [11]. Its diverse applications include drug and protein delivery systems, as well as aid in wound healing [12,13]. An example of such a biomaterial is the extract of *Rhizophora mangle* (*R. mangle*, or red mangrove), a subtropical and tropical plant that is the most abundant vegetation in Brazilian mangroves [14,15]. *R. mangle* has been widely used in folk medicine for its pharmacological properties, which are attributed to its constituent compounds, including tannins and flavonoids—two types of polyphenols which belong to distinct structural classes [16]. Tannins are larger, non-flavonoid polyphenols, generally subdivided into hydrolyzable and non-hydrolyzable types based on their core structure and linkages [73–75]. Flavonoids, in contrast, are water-soluble compounds featuring a specific two-benzene-ring structure [73,76]. Together, these compounds provide *R. mangle* with anti-inflammatory, antioxidant, antimicrobial, and antibacterial properties [17,18], and also regulate tissue regeneration through angiogenesis and increased fibroblast proliferation [8,19]. Among the plant's polyphenolic compounds, tannic acid (TA) is the hydrolysable tannin with the simplest structure [18,20]. TA is known to possess beneficial chemical properties and functional capabilities, including biocompatibility [21], antioxidant, antimicrobial, and antiviral activity [59], and the ability to modulate growth factors and inflammatory cytokines, among others [19,22].

In parallel, hydrogels have gained prominence in biomedical applications. They consist of three-dimensional polymeric networks (either natural or synthetic) and are flexible, cross-linked, hydrophilic or amphiphilic materials capable of retaining large amounts of water or biological fluids [12,23], being remarkably versatile and are frequently studied and used, especially as controlled release systems [24,25]. Alginate (ALG) is an example of a linear anionic biopolymer commonly used in hydrogel form (ALGgel) [6], and widely analyzed in the literature for possessing relevant properties such as biodegradability, biocompatibility, low toxicity, and moldability [26]. Other prominent controlled release systems include Metal-Organic Frameworks (MOFs), which are porous materials with a hybrid three-dimensional crystalline structure formed by metal ions as connectors and organic molecules as linkers [27,28]. Zeolitic Imidazolate Frameworks (ZIFs) are a subcategory of MOFs composed of zinc ions and imidazolates [29,30]. One such MOF is ZIF-8 (Zeolitic Imidazolate Framework-8), widely considered for biomedical applications as a drug carrier [31,32].

The materials *R. mangle*, TA, ALGgel, and ZIF-8 exhibit properties that may contribute to preventing necrosis in ISFs by promoting antioxidant, angiogenic, anti-inflammatory, and controlled drug release effects. Recent advancements suggest that combining hydrogels with MOFs like ZIF-8 can create delivery systems with synergistic advantages, which could potentially enhance compound stability and provide controlled release kinetics [64–67]. In the present study's approach, the alginate forms the primary matrix while the incorporated ZIF-8 is intended to function as a drug delivery system (DDS), leveraging the distinct effects of both *R. mangle* and TA for optimized local delivery. Thus, this study aimed to evaluate the potential of novel alginate-ZIF-8 hydrogel systems, enriched with either *R. mangle* extract or TA, to prevent tissue necrosis in a rat model.

Materials and methods

Study design

This is an *in vivo* experimental or interventional study.

Experiment performed

The animals were subjected to a surgical procedure to create an ISF, based on the division of the experimental groups (Box 1). Fig. 1 shows the experimental flowchart detailing the steps of the study.

Study location and period

The study was conducted through the Graduate Program in Morphotechnology (PPGM), at the Department of Histology and Embryology of the Biosciences Center of the Federal University of Pernambuco (DHE – CB/UFPE). The biomaterials were obtained and prepared at the Morphotechnology Laboratory (Lab Morfotec – DHE) and the Rare Earth Laboratory (BSTR) of the Department of Fundamental Chemistry (DQF) of the Exact and Natural Sciences Center (CCEN/UFPE). The experimental animals were acquired and housed at the Department of Physiology and Pharmacology Bioterium (DFF) of CB/UFPE. The surgical procedures, photography, and collection of tissue samples took place at the Neuroendocrinology and Metabolism Laboratory (DFF – CB/UFPE). Finally, the descriptive, morphometric, histomorphometric, and statistical analyses, as well as the histological preparation of the samples and the taking of photomicrographs, were performed at the Morphotechnology Laboratory (DHE – CB/UFPE).

Research materials

Experimental animals

The study began with 24 male Wistar rats from the same reproductive line aging between 8 and 12 weeks and weighing 220–275 g, which were randomized into four groups ($n = 6$ per group). During the experimental period, two animals from different treatment groups were excluded from the study due to unforeseen complications. Therefore, the final analysis was conducted on a total of 22 animals, with the final number per group detailed in Box 1. The growing animals were kept in groups of up to 5 rats per cage in the bioterium. After the flaps were created, the rats were housed in individual cages with temperature control (22 °$C \pm 2$ °C) and protection from stress and noise, in order to prevent cannibalism of necrotic areas among the animals. Day and night cycles (12/12 h) were maintained, with a standardized diet of industrial chow (Labina Purina Brasil®) and mineral water *ad libitum*, following

Box 1
– Experimental groups with their respective administered treatments and final number (n) of animals per group.

Group	Final n	Administration
NegC	6	0,9 % Saline
pALGgel	5	ALGgel
ALGzTA	5	ALG-ZIF-8 hydrogel system with 5 % TA (ALGzTA-gel)
ALGzRm	6	ALG-ZIF-8 hydrogel system with 5 % *R. mangle (ALGzRm-gel)*

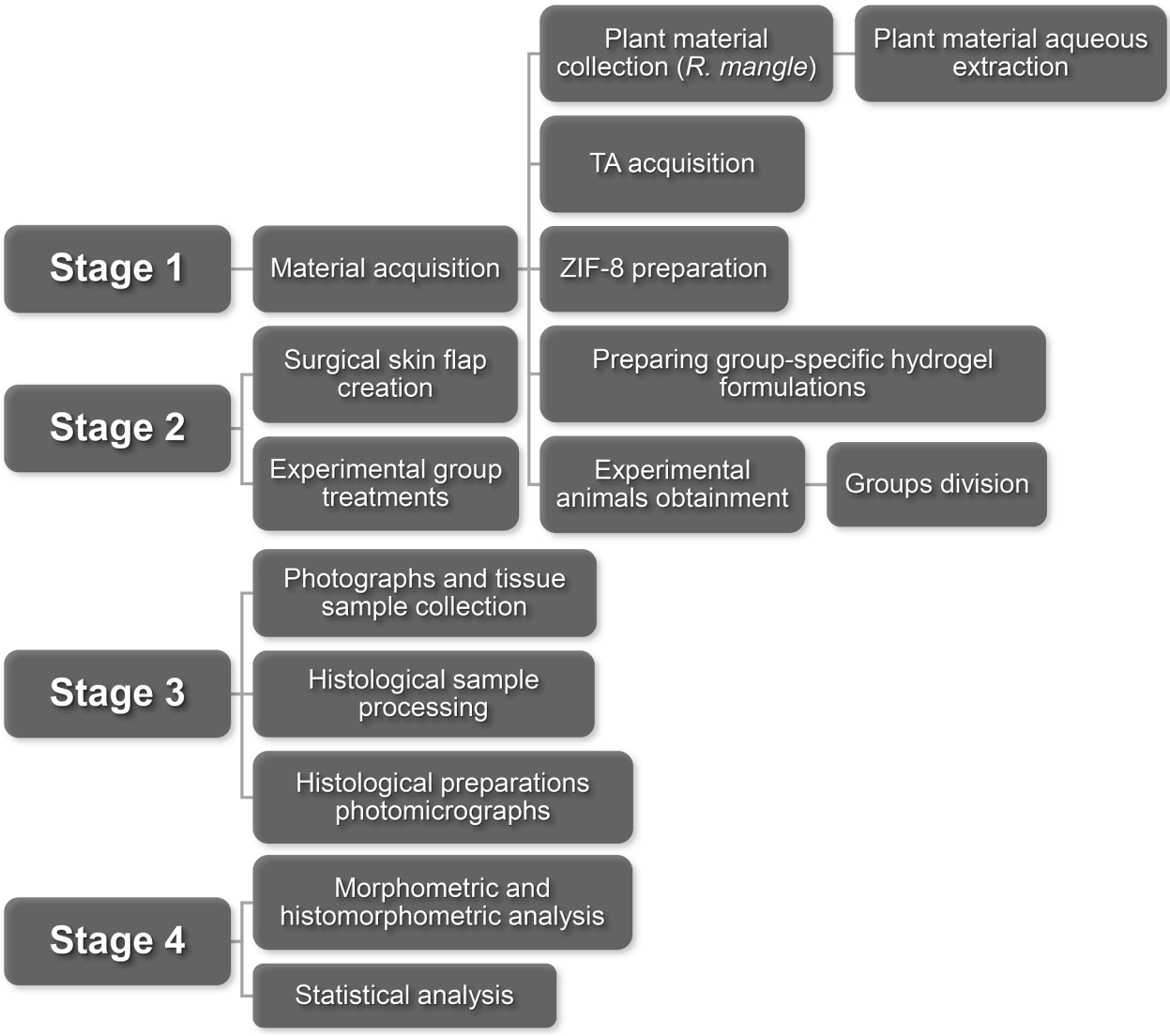

Fig. 1. – Experimental flowchart.

the method applied by Silva *et al.* [5]. The choice of Wistar rats was based on their common availability, low genetic variability, and easy handling, making them a well-validated model for this type of study [63].

Surgical procedure

To carry out the study, surgical procedures were performed on each animal dorsum to create the ISFs. According to Oliveira *et al.* [6], the width of the pedicle and the length of the flap are directly related to its viability. Thus, this work used the same skin flap model utilized by Oliveira [8]. and Silva *et al.* [5], presented by McFarlane, DeYoung, & Henry [33]. and adapted by Adamson *et al.* [34]. Necrosis in the McFarlane random-pattern flap model is triggered by the interruption of the direct blood supply, creating a zone of distal ischemia. The 3:1 length-to-width ratio is specifically designed to exceed the pedicle's perfusion capacity, resulting in predictable necrosis at the flap's extremity. This feature makes the model a standard for evaluating therapeutic strategies aimed at improving flap viability [5,8,33].

At the beginning of the procedure, the animals were weighed and anesthetized with a solution of 30 mg ketamine and 15 mg/kg xylazine intraperitoneal injection, with periodic supplementation, if necessary, in accordance with the animal experimentation ethical principles. Next, trichotomy was performed on animals' dorsal region, with a 3 cm wide base originating from the posterior prominences of the hip and extending 9 cm cranially, such that the occurrence of necrosis becomes predictable [5]. The surgical area was prepared using a 2 % chlorhexidine solution. Subsequently, an incision was made along the marked area, from the base to the extremities down to the superficial fascia, also called *panniculus carnosus*. Following flap elevation and hemostasis, the flap was sutured back onto the wound bed with 3–0 nylon thread. The animals were then sent to their cages for the experiment to begin.

Biomaterials

Plant material collection

R. mangle leaves were collected from the mangrove in the Itamaracá city, Vila Velha district, in the state of Pernambuco – Brazil, at 7° 40‘ south latitude and 34° 50′ west longitude. Green leaves with a healthy appearance, visually intact, and free from mechanical damage, pests, diseases, or altered color were selected. A voucher specimen was identified under number UFP. 69.655.

R. mangle aqueous extract

The aqueous extract of *R. mangle* was obtained at the Lab Morfotec (DHE – CB/UFPE). The extract was prepared by infusion (40 °C for 10 min) from 500 g of previously dried leaves (at 35 °C for 72 h), which

were ground to 0.177 mm in a Pulverisette 14 Classic Fine knife mill (Fritsch). The material was filtered and stored at 5 °C. The phytochemical characterization descriptions of this extract can be found in the works of Oliveira [8]. and Sá *et al.* [15].

Tannic acid

TA in a water-soluble powder form was commercially purchased (Dinâmica® brand) and stored at room temperature in the Morphotechnology Laboratory (DHE – CB/UFPE). At the BSTR Laboratory (DQF – CCEN/UFPE), the TA was diluted to 5 % and incorporated into the ALG-ZIF-8 hydrogel system.

ZIF-8

The ZIF-8 synthesis was based on the methodologies described by Silva [30]. and Hoseinpour and Shariatinia [35], and modified. The preparation took place at the BSTR Laboratory. Two solutions were prepared differently before being mixed. For the first solution, 1.340 g of zinc nitrate hexahydrate ($Zn(NO_3)_2 \bullet 6H_2O$) from Dinâmica® was weighed and placed under agitation with 80 mL of methanol until the metal was completely dissolved. For the second solution, 0.334 g of the 2-methylimidazole (2-MeIM) ligand from Sigma-Aldrich® was weighed and placed under agitation with 80 mL of methanol until completely dissolved. After dissolution, the ligand was added to the metal and kept under agitation for 10 min, then left to rest for 24 h. The resulting solution was separated and washed. Three centrifugations were performed at 3248 g and 5000 RPM for 15 min, where the supernatant was discarded and the material was resuspended in methanol, then again left to rest for 24 h. The yield of the preparation was 0.0296 g, equivalent to 8.86 % of the ligand used. Two other preparations were created seeking to increase the yield, without changes in the preparation method. In the second preparation, the first solution contained ~2.512 g of $Zn(NO_3)_2 \bullet 6H_2O$ diluted in 150 mL of methanol, while the second solution contained ~0.626 g of 2-MeIM diluted in 150 mL of methanol. In the third preparation, the first solution had 1.468 g of $Zn(NO_3)_2 \bullet 6H_2O$ diluted in 100 mL of methanol, while the second solution had 1.620 g of $Zn(NO_3)_2 \bullet 6H_2O$ diluted in 100 mL of methanol. The yields of the second and third preparations were 0.0456 g (equivalent to 7.28 % of the ligand) and 0.376 g (equivalent to 25.6 % of the ligand), respectively.

ALGgel

The formulation containing the ALG hydrocolloid was based on and adapted from the methodology described in the work of Diniz *et al.* [36], where commercially acquired reagents were used without purification: 24 g of ALG from Sigma-Aldrich®, 0.2 g of 1-ethyl-3-(3-dimethylaminopropyl)carbodiimide (EDC) from Sigma-Aldrich®, and 0.06 g of N-hydroxysuccinimide (NHS) from Alfa Aesar®; for 200 mL of ultrapure water from a Milli-Q Direct-Q Type I system from Merck®. In a beaker, a solution containing a concentration equivalent to 12 % (w/v) of ALG in water was created, along with EDC and NHS, which act as coupling agents to control the hydrogel's cross-linking rate. The solution remained under mechanical stirring for 2 h at room temperature. At the end of the stirring period, the hydrogel was stored in a refrigerator.

ALG-ZIF-8 hydrogel system with 5 % TA

For this study, only a single TA concentration was tested, with was set at 5 % based on Guimarães [51]. The formulation containing 5 % TA in the ALG-ZIF-8 hydrogel system was based on and adapted from the methodology described by Diniz *et al.* [36], where commercially acquired reagents were used without purification: 12 g of ALG from Sigma-Aldrich®, 0.2 g of EDC from Sigma-Aldrich®, 0.06 g of NHS from Alfa Aesar®, 0.05 g of ZIF-8, and 5 g of TA; for 100 mL of ultrapure water from a Milli-Q Direct-Q Type I system from Merck®. In a beaker, a solution was created containing a concentration equivalent to 12 % (w/v) ALG, 5 % (w/v) TA, and 0.05 % (w/v) ZIF-8 in water, along with EDC and NHS, which act as coupling agents to control the hydrogel's cross-linking rate. The solution remained under mechanical stirring for 2 h at room temperature. At the end of the stirring period, the hydrogel was stored under refrigeration.

ALG-ZIF-8 hydrogel system with 5 % R. mangle

The concentration (5 %) of *R. mangle* was based on a dose-response study conducted by Silva et al. [5]. The formulation containing 5 % *R. mangle* in the ALG-ZIF-8 hydrogel system was based on and adapted from the methodology described in the work of Diniz et al. [36], where commercially acquired reagents were used without purification: 12 g of ALG from Sigma-Aldrich®, 0.2 g of EDC from Sigma-Aldrich®, 0.06 g of NHS from Alfa Aesar®, and 0.05 g of ZIF-8; for 5 mL of *R. mangle* extract and 95 mL of ultrapure water from a Milli-Q Direct-Q Type I system from Merck®. In a beaker, a solution was created containing a concentration equivalent to 12 % (w/v) of ALG, 5 % (v/v) of *R. mangle*, and 0.05 % (w/v) of ZIF-8 in water, along with EDC and NHS, which act as coupling agents to control the hydrogel's cross-linking rate. The solution remained under mechanical stirring for 2 h at room temperature. At the end of the stirring period, the hydrogel was stored in a refrigerator.

Experimental groups

The animals were randomized into four experimental groups. The designation for each group, number of animals, and specific substance administered are detailed in Box 1. All groups, except for the NegC group, underwent 7 days of topical treatment with their respective hydrogel. Afterward, the animals were euthanized for descriptive, morphometric and histomorphometric analysis of the ISFs. The 7-day treatment period allows for clear demarcation of necrotic and viable tissue, a standard practice in the field [5,59–61]. The study was designed in accordance with the 3Rs principle (Replacement, Reduction, and Refinement) for the ethical use of experimental animals, as endorsed by international guidelines from the OECD [57,58]. Specifically, adhering to the Reduction principle, the sample size of $n = 5–6$ per group was chosen as the minimum number required to achieve statistically robust results while minimizing animal use. This number is consistent with similar published studies in the field, which have demonstrated its sufficiency for detecting significant differences [59–62].

Descriptive analysis of ISFs

At the 7-day endpoint, viable and necrotic areas were macroscopically differentiated. The viable tissue was characterized by its color, texture, hair and scab, while the necrotic tissue was identified by its color, texture and hair.

Morphometric and histomorphometric analyses

At the end of the 7-day post-operative period, the flaps were examined. The necrotic area was macroscopically delineated, and viable tissue was differentiated from necrotic tissue based on texture, color, and hair growth. Additionally, the flaps were photographed, and the images were analyzed for digital measurement using ImageJ software to calculate the percentage of both the necrotic and viable areas relative to the total flap area. Subsequently, the transition zone between the viable and necrotic tissue from each animal was excised and stored for histological preparation. The resulting histological slides were photomicrographed at 20x magnification with PrimeCam 5.1 software and examined. For analysis, five photomicrographs were captured from a specific region of each sample, just above the superficial fascia bordering the necrotic area. In these images, fibroblasts, blood vessels, and leukocytes were counted in five fields per animal using ImageJ software. All animals were euthanized with an anesthetic overdose following tissue collection.

Statistical analysis

The data were analyzed descriptively by the statistical measures: mean, standard deviation (mean ± SD), median, and percentiles 25 and 75 (median (P25; P75)). For comparison between groups, the Student's *t*-test was used with the Kruskal-Wallis test, and in the case of a significant difference, multiple comparison tests (between pairs of groups) by Conover [37]. were obtained. The choice of the Kruskal-Wallis test was due to the sample size in each group being less than 8 cases per group, or the rejection of data normality in at least one of the groups. The normality was verified using the Shapiro-Wilk test [38]. The significance level for all statistical tests was set at 5 % ($p < 0.05$). A power calculation revealed a statistical power of 85.2 %, based on the main variables (viable area, leukocyte, and blood vessel counts) and a 5 % significance level, calculated using G*Power software (version 3.1.9.4). The data were entered into an EXCEL spreadsheet and the program used to obtain the statistical calculations was IBM SPSS version 27.

Results

Obtaining the hydrogels

Fig. 2 shows the three hydrogel formulations that were obtained. The ALGgel (Fig. 2a) presented a translucent coloration and a semi-fluid consistency. Meanwhile, the ALGzTA-gel (Fig. 2b) showed a brown color and a thicker consistency compared to the pure hydrogel. The ALGzRm-gel (Fig. 2c) presented a slightly brownish coloration, tending towards beige, with a more translucent appearance and a more fluid texture when compared to the other formulations.

Descriptive analysis of ISFs

The qualitative macroscopic findings for both the viable and necrotic areas of the flaps are summarized in Table 1. In the viable area, a soft texture was consistently observed across all experimental groups. In terms of color, the pALGgel group was distinct, showing a light red appearance in the majority of animals, while the NegC, ALGzTA, and ALGzRm groups all presented a light beige color. A key difference was noted in hair regrowth, which was present in the control groups (NegC and pALGgel) but absent in the treatment groups (ALGzTA and ALGzRm). Regarding scab formation, a scab was present in the NegC, pALGgel, and ALGzRm groups, but was notably absent in most animals of the ALGzTA group. The necrotic areas showed uniform characteristics across all groups, consistently presenting as black, hard, and with a complete absence of hair.

Morphometric analysis

At the end of the procedure, the flaps from each group were photographed and analyzed. It was observed that the necrotic area had a dark coloration, hardened texture, irregular surface, and absence of hair growth, while the viable area presented a light-red color, soft texture, and the beginning of hair growth (Fig. 3).

Table 2 presents the descriptive statistics for the viable area/total area and necrotic area/total area variables. Although no significant difference was observed between the groups, the ALGzTA group notably had the lowest mean and median percentage of viable area relative to the total area (58.92 % and 71.98 %, respectively). Among the other groups, the ALGzRm group showed the highest mean viable area (87.48 %; median 92.45 %), followed by the NegC group (82.68 %; median 84.73 %) and the pALGgel group (81.07 %; median 81.87 %). Regarding the percentage of necrotic area relative to the total area, the highest mean and median were also recorded in the ALGzTA group (41.08 % and 28.04 %, respectively). In contrast, the ALGzRm group had the lowest mean necrosis (12.52 %; median 7.55 %), followed by the NegC (17.32 %; median 15.27 %) and pALGgel groups (18.93 %; median 18.13 %). Graph 1 highlights the mean percentages of viable and necrotic areas relative to the total area for each experimental group, providing a graphical comparison between the groups. Notably, two of the animals in the ALGzRm group showed total flap viability, with no occurrence of necrosis, after the 7-day experimental period, as shown in the representative example in Fig. 3d

Histomorphometric analysis

After obtaining the histological slides, five fields were photographed from each sample for fibroblast, blood vessel and leukocytes counting. Fig. 4 shows a representative field for each experimental group.

Table 3 presents the descriptive statistics for fibroblast, blood vessel, and leukocyte counts per field for each group. Regarding the fibroblast count per field, no statistically significant difference was found between the groups ($p = 0.192$). The ALGzTA group showed the highest mean (542.68; median 499.00), while the pALGgel group had the lowest (392.96; median 387.00). The NegC and ALGzRm groups exhibited

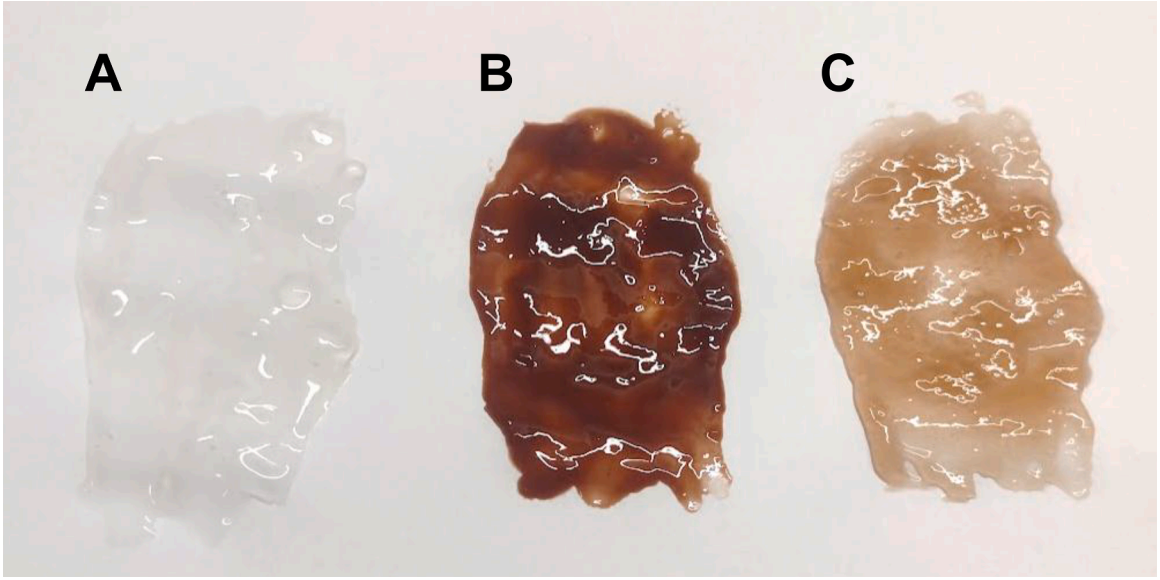

Fig. 2. – Obtained hydrogel formulations. a. ALGgel. b. ALGzTA gel. c. ALGzRm gel.

Table 1
– Descriptive analysis of the ISF qualitative variables by experimental group.

	Qualitative variable						
	Viable area				Necrotic area		
Group	Color	Texture	Hair	Scab	Color	Texture	Hair
NegC	Light beige	Soft	Regrowth	Presence	Black	Hard	Absence
pALGgel	Light red*	Soft	regrowth	Presence	Black	Hard	Absence*
ALGzTA	Light beige	Soft	Absence	Absence*	Black	Hard	Absence
ALGzRm	Light beige	Soft	Absence	Presence*	Black*	Hard*	Absence*

(*) Most part of the group (4 or more animals).

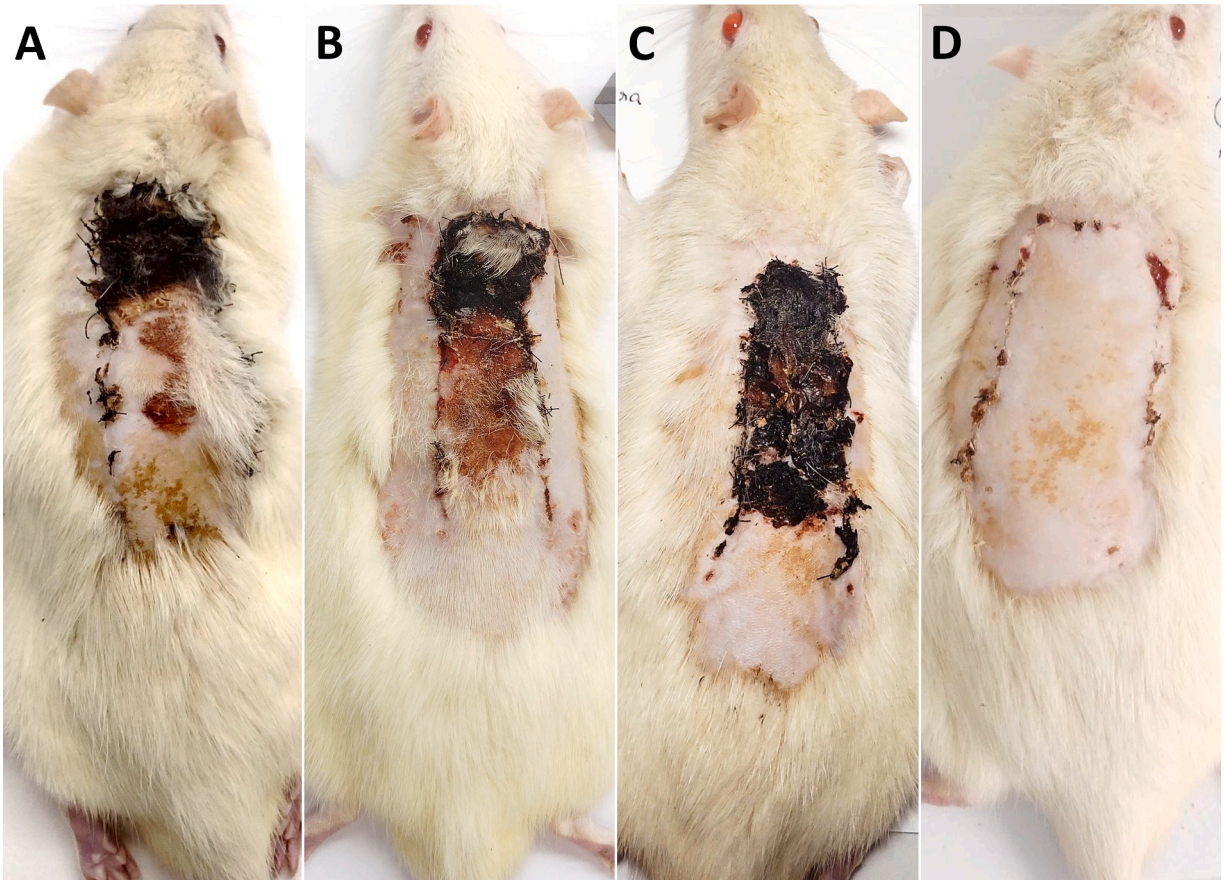

Fig. 3. – Macroscopic analysis of the animals' skin flaps (one specimen per group). a. NegC group. b. pALGgel group. c. ALGzTA group. d. ALGzRm group.

Table 2
– Descriptive statistics of viable and necrotic area percentages relative to the total area, per experimental group.

		Variable	
Group	n	Viable area/total area (%) Mean ± SD Median (P25; P75)	Necrotic area/total area (%) Mean ± SD Median (P25; P75)
NegC	6	82,68 ± 7,83 84,73 (75,21; 89,31)	17,32 ± 7,83 15,27 (10,69; 24,79)
pALGgel	5	81,07 ± 2,68 81,87 (78,27; 83,47)	18,93 ± 2,64 18,13 (16,53; 21,66)
ALGzTA	5	58,92 ± 27,37 71,96 (29,31; 82,00)	41,08 ± 27,40 28,04 (18,05; 70,78)
ALGzRm	6	87,48 ± 14,47 92,45 (70,04; 100,00)	12,52 ± 14,45 7,55 (0,00; 29,95)
P-value		$p^{(1)} = 0214$	$p^{(1)} = 0214$

(1) Kruskal-Wallis Test.

similar means (434.07 and 431.27, respectively) and medians (398.50 and 422.50, respectively). For the number of blood vessels per field, a significant difference was identified between the groups ($p = 0.015$). The highest mean was observed in the ALGzTA group (39.16; median 40.00), followed by the NegC (36.30; median 28.50), ALGzRm (30.17; median 26.50), and pALGgel groups, which had the lowest mean (22.36; median 20.00). As for the leukocyte count per field, the difference between the groups was also significant ($p < 0.001$). The pALGgel group exhibited the highest mean (160.04; median 83.00), whereas the ALGzRm group had the lowest (33.07; median 29.00). The NegC and ALGzTA groups had mean counts of 100.27 and 106.52, with medians of 81.50 and 94.00, respectively.

Graphs 2, 3, and 4 provide a visual representation of the histomorphometry data presented in Table 3, facilitating comparison between evaluated groups. Graph 2 shows the mean fibroblast count per field, highlighting that the ALGzTA group had the highest mean (542.68), followed by the NegC (434.07), ALGzRm (431.27), with the pALGgel group having the lowest mean (392.96). Graph 3 displays the mean blood vessel count per field, with the ALGzTA group again

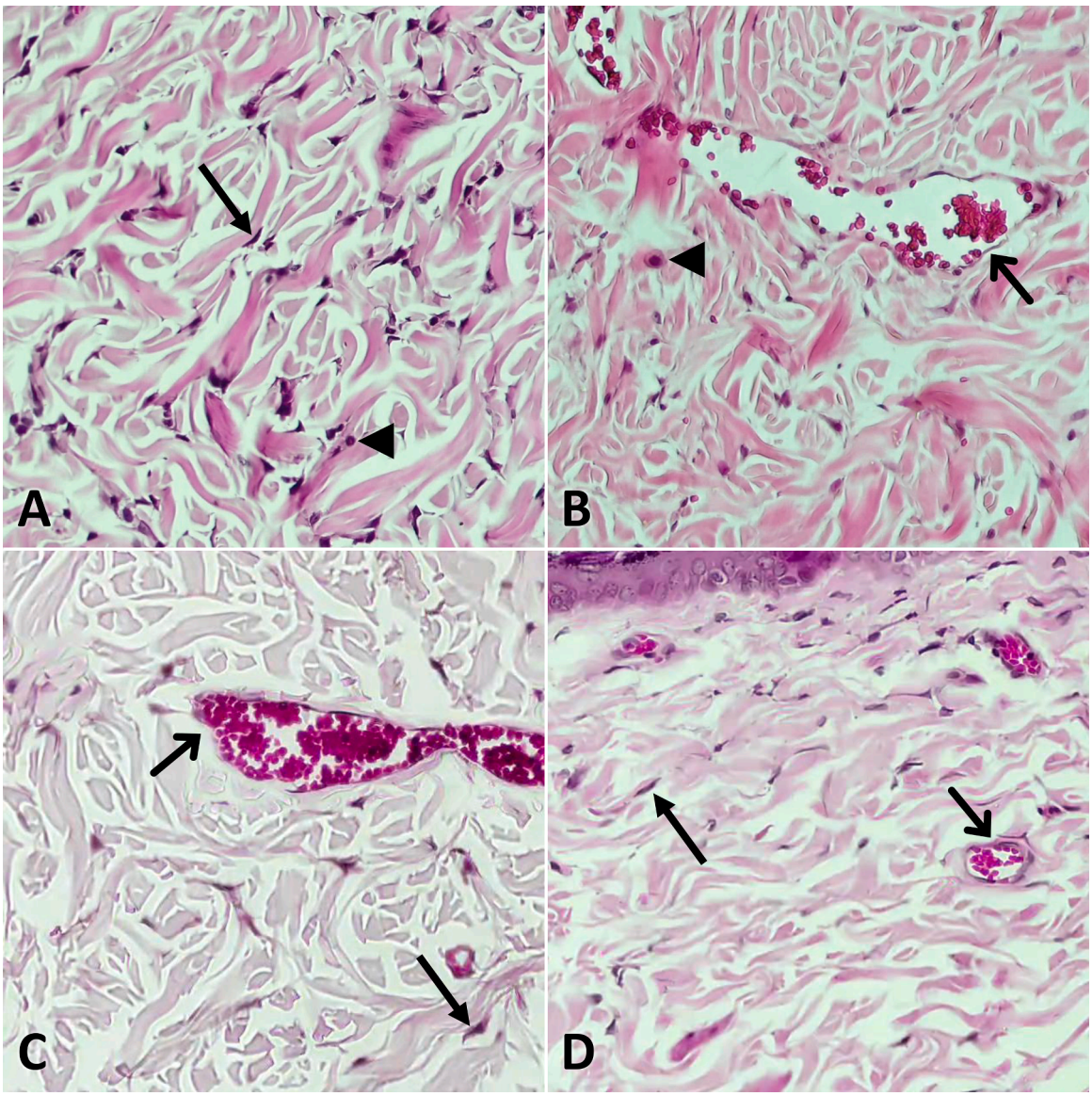

Fig. 4. – Representative histological fields of the experimental groups (20x magnification, H&E stained). a. NegC group. b. pALGgel group. c. ALGzTA group. d. ALGzRm group. Solid arrows in A, C, and D indicate fibroblasts. Open arrows in B, C, and D indicate blood vessels. Arrowheads in A and B indicate leukocytes.

showing the highest mean (39.16), followed by the NegC (36.30) and ALGzRm (30.17) groups, while the pALGgel group had the lowest mean at 22.36. Graph 4 presents the mean leukocyte count per field, with the pALGgel group showing the highest mean (160.04), followed by the ALGzTA (106.52) and NegC (100.27) groups, ending with the ALGzRm group, which had the lowest mean of 33.07.

Discussion

The viability of skin flaps, a frequent procedure in plastic and reconstructive surgery, is constantly threatened by the risk of tissue necrosis in ISFs. This clinical challenge drives the search for new therapeutic strategies, with a special interest in naturally derived compounds. Previous studies have demonstrated the beneficial effect of *R. mangle* extract on the viability of ISFs [5,8]. Additionally, the pioneering study by Marinho [19]. combined *R. mangle* with TA in a cream base for wound treatment, showing favorable healing potential. Similarly, the study by Silva *et al.* [5]. applied the *R. mangle* extract in a hydrogel form, which also yielded a positive result. In this context, natural polymer-based hydrogels stand out as promising vehicles, given their similarity to biological tissues and their capacity to act as controlled release systems for bioactive compounds [23,25]. Building upon the potential of hydrogel vehicles, recent advancements highlight the combination of hydrogels with MOFs like ZIF-8 to create more sophisticated delivery platforms. Such composite systems have suggested benefits including controlled and sustained release kinetics [64], enhanced compound stability and bioavailability [64,65], and the potential for multifunctionality by modulating the local microenvironment [66], with MOFs appearing to remain stable and functional when embedded within the hydrogel matrix [67]. Therefore, the present study evaluated the potential of different ALG-ZIF-8 hydrogel systems in preventing tissue necrosis in ISFs, using ALGgel as the primary matrix, and incorporating ZIF-8 as a DDS, aiming to enhance the effects of *R. mangle* and TA.

The morphometric analysis in the present study demonstrated clear trends regarding the potential of the different hydrogel formulations to influence necrosis prevention. Although differences were observed in the means, there was no statistically significant difference between the groups ($p = 0.214$), which may be attributed to high data variability. Accordingly, the results suggest that treatment with ALGzRm-gel was

Table 3
– Statistics of fibroblast, blood vessel, and leukocyte counts per field, for each experimental group.

		Variable		
		Fibroblasts/field	Blood vessel/field	Leukocyte/field
Group	n	Mean ± SD Median (P25; P75)	Mean ± SD Median (P25; P75)	Mean ± SD Median (P25; P75)
NegC	30	434,07 ± 159,38	36,30 ± 49,94 (AB)	100,27 ± 73,71 (A)
		398,50 (327,25; 516,00)	28,50 (15,50; 40,25)	81,50 (55,50; 117,75)
pALGgel	25	392,96 ± 124,34	22,36 ± 15,94 (A)	160,04 ± 179,37 (A)
		387,00 (294,00; 501,50)	20,00 (6,50; 35,00)	83,00 (26,00; 228,50)
ALGzTA	25	542,68 ± 259,56	39,16 ± 19,27 (B)	106,52 ± 70,99 (A)
		499,00 (396,50; 646,00)	40,00 (18,50; 53,50)	94,00 (70,50; 122,50)
ALGzRm	30	431,27 ± 119,31	30,17 ± 15,19 (A)	33,07 ± 24,73 (B)
		422,50 (313,75; 531,75)	26,50 (17,75; 39,75)	29,00 (16,00; 39,75)
P-value		$p^{(1)} = 0192$	$p^{(1)} = 0015$*	$p^{(1)} < 0001$*

(*) Significant difference at 5,0 % level.
(1) Kruskal-Wallis test with Conover's multiple comparisons test.
Note: Groups that do not share a common letter in parentheses are significantly different.

associated with the most favorable outcomes. As detailed in Table 2 and illustrated in Graph 1, the ALGzRm group achieved the highest mean flap viability (87.48 %). This trend was also evident in the macroscopic analysis, where animals in this group presented flaps with an excellent appearance, including two cases of complete absence of necrosis (Fig. 3d). These observations may be related to the well-known properties of the *R. mangle* extract, such as its antioxidant, anti-inflammatory, healing, and angiogenic effects [43,44]. The findings of this study are consistent with previous studies that have demonstrated the therapeutic potential of the extract in different formulations, such as creams, films, and hydrogels [8,14,45]. They also align with the work of Silva *et al.* [5], whose results showed decreased necrosis with a 5 % *R. mangle* hydrogel, a trend similarly observed in the present study, though not statistically significant for the primary endpoint.

Furthermore, the favorable trends observed in the ALGzRm group may be partly attributed to the presence of ZIF-8 in the tested formulation. In the study by Silva *et al.* [5], a mean necrosis of 34.25 % was reported in the group that tested a xanthan gum hydrogel with 5 % *R. mangle* extract. In contrast, this value is substantially higher than that found in the present study for the ALGzRm group (12.52 %), which used the same extract concentration. This difference raises the hypothesis that the inclusion of ZIF-8 could potentially enhance the therapeutic effects of the *R. mangle* extract, possibly by acting as a DDS and optimizing the formulation. This also suggests a potential synergistic effect within the ALGzRm-gel, where the ALG-ZIF-8 hydrogel system likely contributed to the outcomes observed. Likewise, ZIF-8 properties as a porous and biocompatible carrier [46]. might have contributed to a more sustained local action, which could explain the significantly improved histological findings related to reduced inflammation and controlled angiogenesis observed in this group.

In contrast, the ALGzTA-gel demonstrated an apparently detrimental effect, resulting in the highest mean necrosis among all groups (41.08 %), while the NegC and pALGgel groups showed intermediate and similar results. This macroscopic observation is corroborated by the histomorphometric findings (Table 3), which indicate an intense inflammatory process in this group, further confirmed by the highest mean blood vessel count (39.16; $p = 0.015$) and a high mean leukocyte count (106.52; $p < 0.001$), both of which were statistically significant (Graph 2), also indicating a process of exacerbated angiogenesis. One hypothesis to explain this negative outcome is the dual behavior of tannins and other polyphenols [47]. Although it is an antioxidant at low concentrations, at higher concentrations TA can become pro-oxidant, increasing ROS generation and inducing cellular damage [48–50].

The results from the NegC and pALGgel groups provide context for the other findings. The NegC group, treated with saline, presented a necrotic area of 17.32 %, a value lower than those observed in the control groups of Oliveira [8]. and Silva *et al.* [5]. (48.88 % and 50.66 %, respectively). Meanwhile, the pALGgel (placebo) group had an 18.93 % necrotic area, a more favorable result than that of the group in Silva *et al.*, which was treated with a xanthan gum hydrogel + placebo (37.44 %). However, a comparison of NegC and pALGgel groups shows that the placebo alone was not able to improve flap viability relative to the negative control.

The histomorphometric analysis performed in this study aids in understanding the events observed in the macroscopic results. This analysis relevance is corroborated by Marinho [19], whose work highlighted

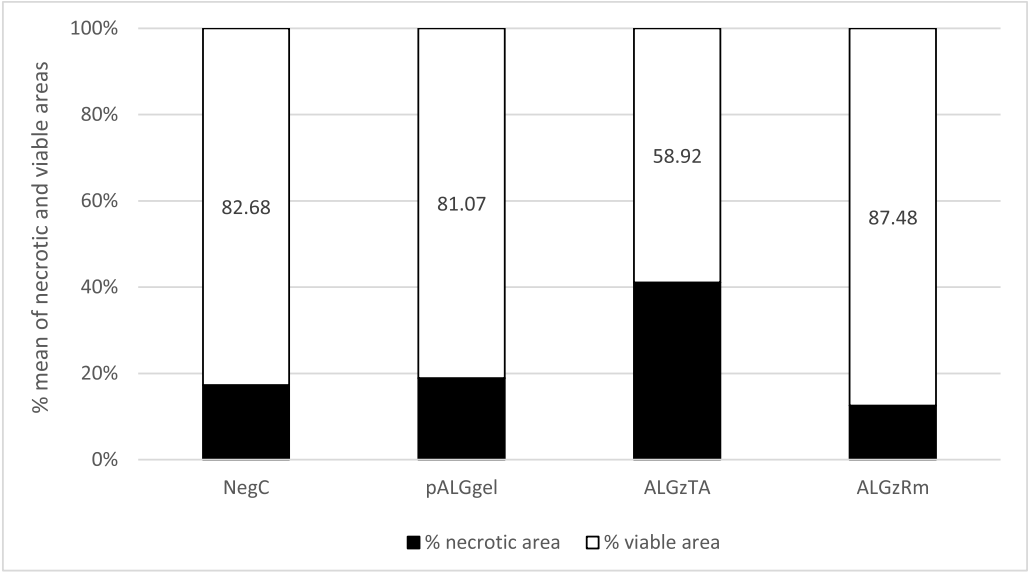

Graph 1. – Mean percentages of the viable and necrotic areas relative to the total area, per experimental group. Note how the viable area predominates in the ALGzRm group, whereas the ALGzTA group exhibits a higher proportion of necrotic area.

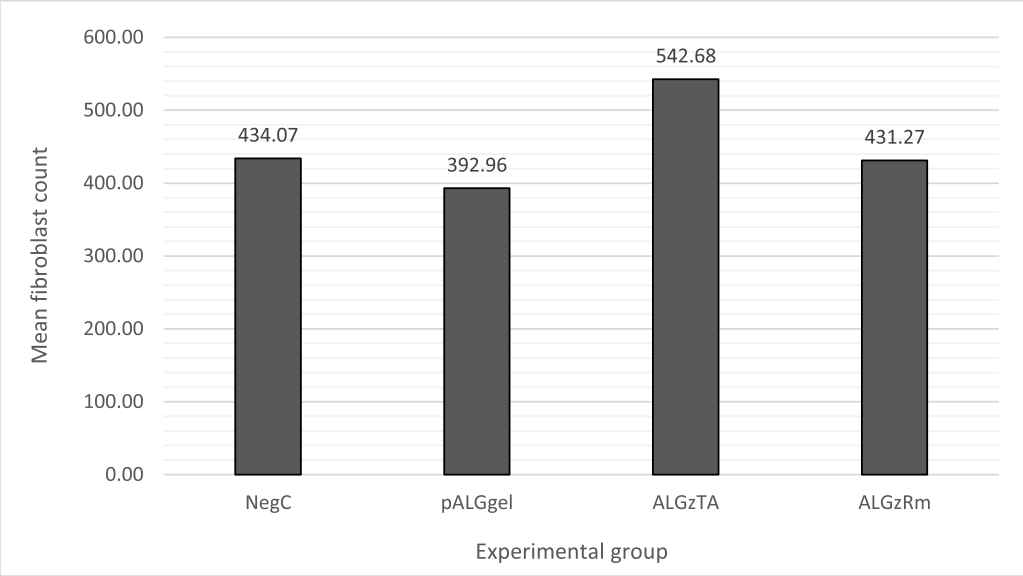

Graph 2. – Mean fibroblast count per experimental group.

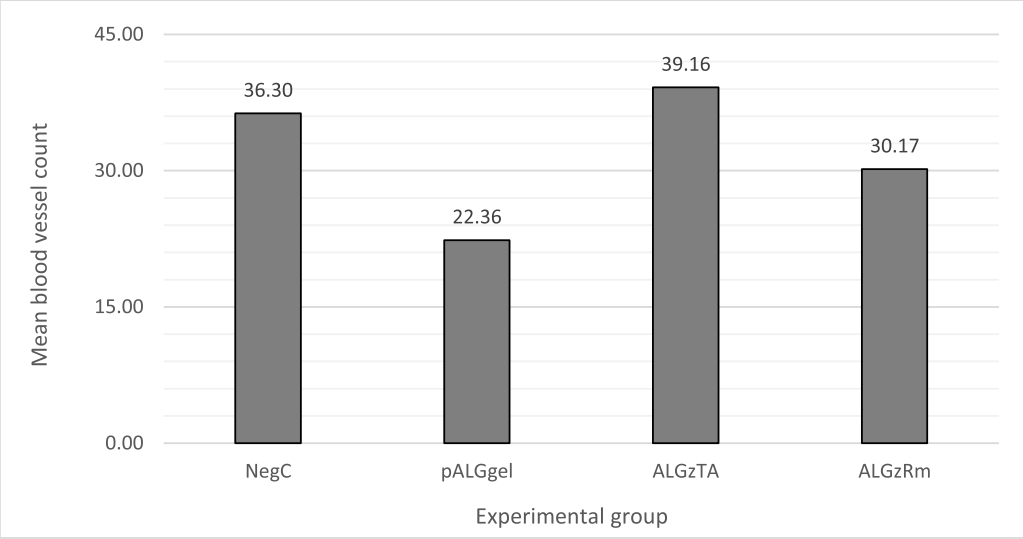

Graph 3. – Mean blood vessel count per experimental group.

histomorphometry as crucial for measuring the tissue repair degree. Although the necrotic areas of NegC and pALGgel groups were smaller than those reported by Oliveira [8]. and Silva *et al.* [5], and the pALGgel group's necrotic area was lower than the observed in Silva *et al.* placebo, the resulting histomorphometry is consistent with a pattern of repair failure in both groups. Both NegC and pALGgel exhibited an intense inflammatory process, supported by high mean leukocyte counts (100.27 and 160.04, respectively), with placebo group showing the highest mean of the entire study, accompanied by pathological angiogenesis, a process often driven by oxidative stress that tends to persist in an uncontrolled and unresolved manner (mean blood vessel counts of 36.30 and 22.36, respectively) [52].

Regarding the fibroblast count, there was no statistical difference between the groups. While fibroblasts are known regulators of wound healing and extracellular matrix production [8,53,54], the lack of significant variation in this study is consistent with previous reports [5,8], and thus suggests that differences in fibroblast numbers were not the primary driver of the observed flap outcomes. Furthermore, in line with Silva *et al.*, the present study found no evidence of stimulated fibroblast proliferation by using formulations containing *R. mangle*.

The blood vessel count, which reflects the process of angiogenesis, revealed a significant difference between the groups ($p = 0.015$), as did the leukocyte count ($p < 0.001$). Thus, a combined analysis of these two variables offers a cellular-level explanation for the macroscopic results previously discussed. The inflammatory response in ALGzTA group is validated by the high leukocyte and blood vessel counts, which are directly associated with pathological angiogenesis, thereby justifying the extensive necrosis. In contrast, the favorable outcome observed in ALGzRm group is due to its potent anti-inflammatory action, confirmed by this study's lowest leukocyte count along with a physiological and controlled angiogenesis, likely contributing to the higher mean flap viability seen in this group.

The choice of 5 % TA concentration was based on Guimarães study [51], who used this same concentration in two formulations (a base gel-cream and an aqueous solution) to evaluate the TA photoprotective effect and to study its fluorescence, permeation, and cutaneous retention *in vitro*. The use of TA in formulations for cutaneous wound treatment was also investigated by Marinho [19], who, however, used a lower

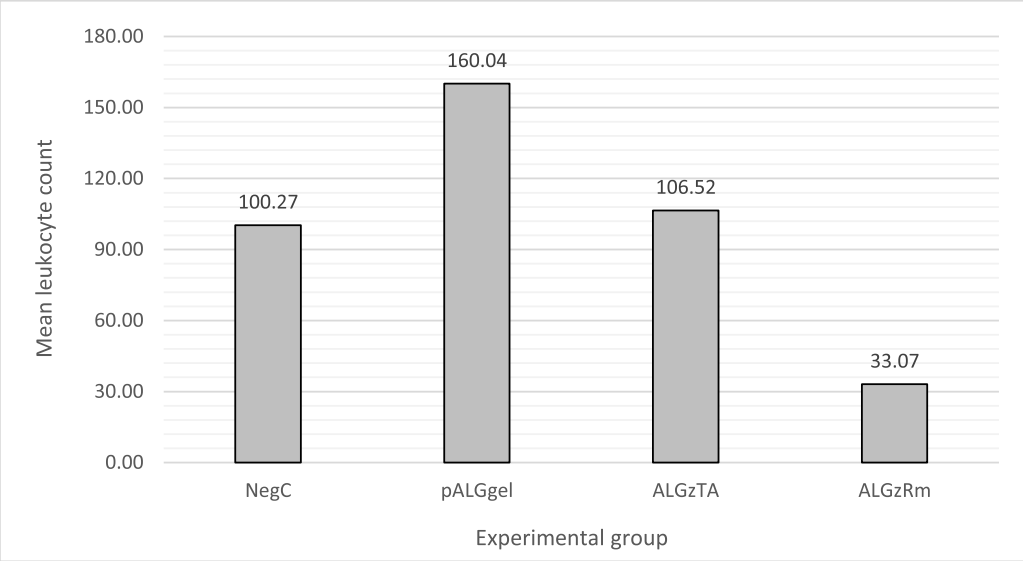

Graph 4. – Mean leukocyte count per experimental group.

concentration of 2.5 % TA in combination with 2.5 % *R. mangle* extract to treat cutaneous wounds. It is relevant to note that, in Marinho's study, the approach combining 2.5 % TA concentration with *R. mangle* extract achieved a positive healing outcome. Meanwhile, the results from Guimarães demonstrated that, without an effective delivery system, TA was retained in the epidermis, failing to reach the deeper layers of the skin. In the present study formulation, however, the presence of ZIF-8 as a DDS likely facilitated TA permeation through the epidermis, effectively delivering what appeared to be a high and pro-oxidant dose directly to the ischemic tissue. This suggests that the combined action of TA with the ALG-ZIF-8 delivery platform in the ALGzTA-gel may have synergistically led to the observed detrimental effects, and would explain the intense inflammatory response and fibroblast proliferation. Indeed, the angiogenesis observed in the ALGzTA group aligns with the characteristics of a pathological process [52], which, combined with the chronic inflammation and fibrosis, likely culminated in tissue death rather than repair. This fact raises the hypothesis that the safe therapeutic concentration for TA is below 5 %, and possibly closer to the 2.5 % used by Marinho. Furthermore, it cannot be ruled out that the *R. mangle* extract present in that formulation may have contributed to attenuating the TA pro-oxidant potential. Thus, the need for future dose-response studies becomes evident to determine the ideal and safe concentration of TA for this application, as well as *in vitro* assays to directly evaluate its oxidative stress potential at different concentrations. Additionally, studies evaluating TA use to prevent necrosis in ISFs were not found in the literature, limiting a comparative discussion of the findings. However, the successful use of *R. mangle*, which contains tannins in its composition [8,15,16], justifies the interest in investigating TA in isolation to improve ISFs viability.

These results represent an advancement over previous works. Silva *et al.* [5], for example, observed a pro-angiogenic trend with *R. mangle* but without statistical significance or a leukocyte count, limiting a more complete interpretation of the phenomenon. Oliveira [8], who evaluated both variables, found no significant difference for either of them. In light of this, the statistically significant results of this work for blood vessel and leukocyte counts indicate a positive biological response elicited by the ALGzRm formulation and elucidate that controlling inflammation is a critical aspect of the angiogenic response quality, which may contribute to improved ISF viability.

This study utilized the McFarlane skin flap model adapted by Adamson *et al.* [33,34], specifically employing the commonly used 3 cm x 9 cm caudally based modification. This version, derived from McFarlane's original model and its variations [39–42], is a well-established standard for investigating ISF necrosis prevention in Wistar rats [5,8]. The macroscopic criteria used in this study for distinguishing viable from necrotic area was detailed in Table 1 and align with those employed by other studies [5,59–61,77,78]. This consistency in assessment standards supports the reliable differentiation between tissue outcomes observed in the present study and allows for comparison across similar flap viability investigations.

The choice to use male rats, contrasting Silva *et al.* [5], who used females, is a notable methodological difference that may have contributed to clarify this study's results. Findings in the literature show that hormones such as estrogen, progesterone, and estradiol are critical mediators that influence wound healing, angiogenesis, and collagen remodeling [55,56]. According to Silva *et al.* [5], the estrous cycle in females may have introduced hormonal variability during the ISFs healing in their study. In this regard, the choice to use male rats in this work, similar to Oliveira [8], represents a methodological advantage, ensuring that the observed outcomes more directly reflect the tested formulations efficacy without interference of hormonal fluctuations.

Some limitations of the present study should be acknowledged. First, a functional assessment of flap perfusion was not performed. Future research would benefit from incorporating techniques like Laser Doppler imaging to dynamically measure blood flow. Additionally, the study did not include a preliminary *in vitro* component. Future investigations are therefore suggested to assess the effects of *R. mangle* and TA on cell lines – such as HUVECs for angiogenic potential, and fibroblasts (NIH/3T3) or keratinocytes (HaCaT) for cytotoxicity and proliferation – as an important preliminary step to optimize formulations before further *in vivo* testing. Furthermore, blinding could only be employed during the histomorphometric and statistical analyses. To better minimize potential bias, future similar studies should aim to implement a more comprehensive double-blinding protocol, including during treatments application.

Conclusion

In conclusion, this study highlights the potential of novel alginate-ZIF-8 hydrogel systems for modulating ischemic flap outcomes. The ALGzRm-gel formulation demonstrated promise for tissue repair, likely mediated by its ability to control the inflammatory response. Conversely, the ALGzTA-gel appeared detrimental, as evidenced by exacerbated inflammation and pathological angiogenesis. The ZIF-8

delivery component likely played a key role in these distinct cellular responses. These findings underscore the translational potential of ALGzRm-gel as a platform for enhancing flap viability. Crucial future steps include investigating the dose-dependent effects of TA to determine its therapeutic window for this application.

Ethics statement

The experiment was conducted according to ARRIVE guidelines. This study was reviewed and approved by the Ethics Committee on the Use of Animals (CEUA) of the Federal University of Pernambuco (UFPE) under protocol number 0072/2023 (Appendix A). The work was conducted with concern for causing the minimum possible suffering to the animals.

CRediT authorship contribution statement

Bianca Rocha da Silva Barreto: Writing – review & editing, Writing – original draft, Visualization, Validation, Supervision, Software, Resources, Project administration, Methodology, Investigation, Funding acquisition, Formal analysis, Data curation, Conceptualization. **Eduardo Carvalho Lira:** Supervision, Resources, Methodology. **Severino Alves Júnior:** Visualization, Supervision, Methodology. **Luzia Abilio da Silva:** Visualization, Supervision, Resources, Methodology, Investigation, Formal analysis. **Yuri José de Albuquerque Silva:** Visualization, Supervision, Software, Resources, Methodology, Formal analysis. **Widarlane Ângela da Silva Alves:** Methodology. **Madson Manoel Nunes da Silva:** Methodology. **Rosallyne Hosana Vanderlei das Chagas:** Methodology. **Larissa Cardeal da Rocha Carvalho:** Methodology. **Jasmine Martins Vieira Cunha:** Methodology. **Jamily Isabel Viana de Lima:** Methodology. **Ester Francisca Gomes de Lima:** Methodology. **Ícaro Mota Oliveira:** Writing – review & editing. **Jeymesson Raphael Cardoso Vieira:** Writing – review & editing, Writing – original draft, Visualization, Validation, Supervision, Software, Resources, Project administration, Methodology, Investigation, Funding acquisition, Formal analysis, Data curation, Conceptualization.

Declaration of competing interest

There are no conflicts of interest in the execution of this work.

References

[1] Casey G. Physiology of the skin. Nurs Stand 2002 May;16(34):47–51.
[2] Alves NC. [Penetração de Ativos na Pele: revisão bibliográfica]. Amazônia Sci Health 2015;3(4):36–43. Portuguese.
[3] Moore KL, Dalley AF, Agur AMR. Clinically oriented anatomy. 7th ed. Philadelphia: Wolters Kluwer Health/Lippincott Williams & Wilkins; 2013.
[4] Arda O, Göksügür N, Tüzün Y. Basic histological structure and functions of facial skin. Clin Dermatol 2014;32(1):3–13.
[5] Silva LA, Lira EC, Leal LB, Santana ES, Barbosa ISF, Silva YJA, et al. Prevention of necrosis in ischemic skin flaps using hydrogel of Rhizophora mangle. Injury 2022; 53(7):2462–9.
[6] Oliveira JAV, Santana ES, Silva LA, Fernandes FHP, Lira EC, Vieira JRC. Ischemic skin flaps: what to use to save them? a narrative review. Rev Foco 2023;16(1): e728. https://doi.org/10.54751/revistafoco.v16n1-033.
[7] Duarte IS, Gomes HFC, Ferreira LM. Effect of dimethyl sulphoxide on necrosis of skin flaps in rats. Can J Plast Surg 1998;6(2):93–7.
[8] Oliveira JAV. Aplicação da Rhizophora mangle associada ao biopolímero de betaglucana em retalhos cutâneos isquêmicos em ratos [dissertation on the Internet]. Recife (PE): Universidade Federal de Pernambuco; 2018.
[9] Pu C, Liu C, Liang C, Yen Y, Chen S, Jiang-Shieh Y, et al. Adipose-derived stem cells protect skin flaps against ischemia/reperfusion injury via il-6 expression. J Invest Dermatol 2017;137(6):1353–62.
[10] Gözü A, Poda M, Taşkin Eİ, Turgut H, Erginel-Ünaltuna N, Doğruman H, et al. Pretreatment with octreotide modulates iNOS gene expression, mimics surgical delay, and improves flap survival. Ann Plast Surg 2010;65(2):245–9.
[11] Williams DF. On the nature of biomaterials. Biomaterials 2009;30(30):5897–909.
[12] Hasirci V, Hasirci N. Fundamentals of biomaterials. New York: Springer; 2018. https://doi.org/10.1007/978-1-4939-8856-3.
[13] Bharadwaj A. An overview on biomaterials and its applications in medical science. IOP Conf Ser Mater Sci Eng 2021;1116(1):012178.
[14] Araújo JG. Desenvolvimento de creme de Rhizophora mangle l: avaliação do potencial cicatrizante em feridas cutâneas [dissertation on the Internet]. Recife (PE): Universidade Federal de Pernambuco; 2015.
[15] Sá JGA, Brandão WFM, Santana MAN, da Silva LA, de Santana ES, da Silva EC, et al. [Avaliação da citotoxicidade e caracterização do perfil fitoquímico de Rhizophora mangle L. do mangue brasileiro]. Ciência e saúde: uma visão integrativa. Seven Editora 2023. p. 528–39. Portuguese.
[16] Lima GC, da Costa MAS, da S Júnior JB, da Silva RB, de Souza IA, de Oliveira AFM, et al. [Phytochemical screening, cytotoxic and genotoxic activity of the aqueous extract of Rhizophora mangle L]. Braz J Dev 2021;7(3):26458–74. Portuguese.
[17] Ferreira FS, Santos SC, Barros TF, Rossi-Alva JC, Fernandez LG. [Atividade antibacteriana in vitro de extratos de Rhizophora mangle L]. Rev Bras Plantas Med 2011;13(3):305–10. Portuguese.
[18] Jing W, Xiaolan C, Yu C, Feng Q, Haifeng Y. Pharmacological effects and mechanisms of tannic acid. Biomed Pharmacother 2022;154:113561.
[19] Marinho AGC. Rhizophora mangle e ácido tânico: uma associação em creme para o tratamento de feridas [dissertation on the Internet]. Recife (PE): Universidade Federal de Pernambuco; 2018.
[20] Brandão LFG, Costa CMD, Lacerda DP, Siqueira JM. [Controle de qualidade do ácido tânico de algumas farmácias de manipulação de Campo Grande (MS), Brasil]. Rev Eletrônica Farm [Internet] 2008;5(3):33–8. https://doi.org/10.5216/ref.v5i3.5369 [cited 2024 Apr 1]Available from, https://revistas.ufg.br/REF/article/view/5369. Portuguese.
[21] Chen C, Yang H, Yang X, Ma Q. Tannic acid: a crosslinker leading to versatile functional polymeric networks. RSC Adv 2022;12(13):7689–711.
[22] Chen Y, Tian L, Yang F, Tong W, Jia R, Zou Y, et al. Tannic Acid Accelerates Cutaneous Wound Healing in Rats Via Activation of the ERK 1/2 Signaling Pathways. Adv Wound Care 2019;8(7):341–54.
[23] Ullah F, Othman MBH, Javed F, Ahmad Z, Akil H. Classification, processing and application of hydrogels: a review. Mater Sci Eng C 2015;57:414–33.
[24] Laftah WA, Hashim S, Ibrahim AN. Polymer Hydrogels: a review. Polym Plast Technol Eng 2011;50(14):1475–86.
[25] Li J, Mooney DJ. Designing hydrogels for controlled drug delivery. Nat Rev Mater 2016;1(12):16071.
[26] Neves RCS. Plataforma multifuncional a base de gel aplicada à terapia fotodinâmica e fototérmica para câncer de pele [dissertation on the Internet]. Recife (PE): Universidade Federal de Pernambuco; 2019.
[27] Cunha DP. Redes de Coordenação: novos sistemas carreadores de fármacos [dissertation on the Internet]. Recife (PE): Universidade Federal de Pernambuco; 2009.
[28] Tanaka S, Kimura Y, Fuku K, Ikenaga N, Nakagawa K. Zinc-imidazole-based metal-organic framework nanosheet membrane for H2/O2 separation. IOP Conf Ser Mater Sci Eng 2024;1318(1):012035.
[29] Tian Z, Yao X, Zhu Y. Simple synthesis of multifunctional zeolitic imidazolate frameworks-8/graphene oxide nanocrystals with controlled drug release and photothermal effect. Microporous Mesoporous Mater 2017;237:160–7.
[30] Silva YJA. Design de ZIF-8-90 bioconjugada para drug delivery no tratamento da tuberculose pulmonar [dissertation on the Internet]. Recife (PE): Universidade Federal de Pernambuco; 2019.
[31] Vasconcelos IB, da Silva TG, Militão GCG, Soares TA, Rodrigues NM, Rodrigues MO, et al. Cytotoxicity and slow release of the anti-cancer drug doxorubicin from ZIF-8. RSC Adv 2012;2(25):9437.
[32] Kaur H, Mohanta GC, Gupta V, Kukkar D, Tyagi S. Synthesis and characterization of ZIF-8 nanoparticles for controlled release of 6-mercaptopurine drug. J Drug Deliv Sci Technol 2017;41:106–12.
[33] McFarlane RM, DeYoung G, Henry RA. The design of a pedicle flap in the rat to study necrosis and its prevention. Plast Reconstr Surg 1965;35(2):177–82.
[34] Adamson JE, Horton CE, Crawford HH, Jr Ayers W. The effects of dimethyl sulfoxide on the experimental pedicle flap: a preliminary report. Plast Reconstr Surg 1966;37(2):105–10.
[35] Hoseinpour V, Shariatinia Z. Applications of zeolitic imidazolate framework-8 (ZIF-8) in bone tissue engineering: a review. Tissue Cell 2021;72:101588.
[36] Diniz FR, Maia RCAP, de Andrade LRM, Andrade LN, Chaud MV, da Silva C, et al. Silver nanoparticles-composing alginate/gelatine hydrogel improves wound healing In Vivo. Nanomaterials 2020;10(2):390.
[37] Conover WJ. Practical nonparametric statistics. 2nd ed. New York: John Wiley & Sons; 1980.
[38] Altman DG. Practical statistics for medical research. London: Chapman And Hall; 1991.
[39] Lee JH, You HJ, Lee TY, Kang HJ. Current status of experimental animal skin flap models: ischemic preconditioning and molecular factors. Int J Mol Sci 2022;23(9): 5234.
[40] Fan W, Liu Z, Chen J, Liu S, Chen T, Li Z, et al. Effect of memantine on the survival of an ischemic random skin flap and the underlying mechanism. Biomed Pharmacother 2021;143:112163.
[41] Luo Z, Bian Y, Zheng G, Wang H, Yan B, Su W, et al. Chemically modified sdf-1α mrna promotes random flap survival by activating the SDF-1α/CXCR4 Axis in Rats. Front Cell Dev Biol 2021;9:623959.
[42] Masaoka K, Asato H, Umekawa K, Imanishi M, Suzuki A. Value of remote ischaemic preconditioning in rat dorsal skin flaps and clamping time. J Plast Surg Hand Surg 2016;50(2):107–10.
[43] Marrero E, Sánchez J, de Armas E, Escobar A, Melchor G, Abad MJ, et al. COX-2 and sPLA2 inhibitory activity of aqueous extract and polyphenols of Rhizophora mangle (red mangrove). Fitoterapia 2006;77(4):313–5.

[44] Fernandez O, Capdevila JZ, Dalla G, Melchor G. Efficacy of Rhizophora mangle aqueous bark extract in the healing of open surgical wounds. Fitoterapia 2002;73 (7–8):564–8.
[45] Santana ES, Leal LB, Silva LA, Barbosa ISF, Melo CML, Santos DKDN, et al. Association of Rhizophora mangle and ascorbic acid in hydrogels: evaluation of cytotoxic and immunomodulatory effects. Braz J Pharm Sci 2023;59:e20179.
[46] Hoop M, Walde CF, Riccò R, Mushtaq F, Terzopoulou A, Chen XZ, et al. Biocompatibility characteristics of the metal organic framework ZIF-8 for therapeutical applications. Appl Mater Today 2018;11:13–21.
[47] Eghbaliferiz S, Iranshahi M. Prooxidant activity of polyphenols, flavonoids, anthocyanins and carotenoids: updated review of mechanisms and catalyzing metals. Phytother Res 2016;30(9):1379–91.
[48] Khan NS, Ahmad A, Hadi SM. Anti-oxidant, pro-oxidant properties of tannic acid and its binding to DNA. Chem Biol Interact 2000;125(3):177–89.
[49] Labieniec M, Gabryelak T, Falcioni G. Antioxidant and pro-oxidant effects of tannins in digestive cells of the freshwater mussel Unio tumidus. Mutat Res 2003; 539(1–2):19–28.
[50] Bouki E, Dimitriadis VK, Kaloyianni M, Dailianis S. Antioxidant and pro-oxidant challenge of tannic acid in mussel hemocytes exposed to cadmium. Mar Env Res 2013;85:13–20.
[51] Guimarães EB. [Efeito fotoprotetor do ácido tânico em gel-creme e estudos de fluorescência, permeação e retenção cutânea in vitro] [dissertation on the internet]. Recife (PE): Universidade Federal de Pernambuco; 2022 [cited 2024 Mar 16]Available from, https://repositorio.ufpe.br/handle/123456789/65677.
[52] Chung AS, Ferrara N. Developmental and pathological angiogenesis. Annu Rev Cell Dev Biol 2011;27:563–84.
[53] Lu WW, Ip WY, Holmes AD, Chow SP, Jing WM. Biomechanical properties of thin skin flap after basic fibroblast growth factor (bFGF) administration. Br J Plast Surg 2000;53(3):225–9.
[54] Mendonça RJ, Coutinho-Netto J. [Aspectos celulares da cicatrização]. Bras Dermatol 2009;84(3):257–62. Portuguese.
[55] Biondo-Simões MLP, Zimmermann E, Daher TS, Borsato KS, Noronha L. [Efeitos da terapia de reposição hormonal na cicatrização de anastomoses de cólon]. Acta Cir Bras 2005;20(3):237–42. Portuguese.
[56] Nicolau JAZ, Faria PF, Marques LO, Hoepers DF, Rocha AD, Sobral ACL. [Análise do efeito do estradiol e progesterona tópicos na cicatrização de feridas em ratos]. Surg Cosmet Dermatol 2014;6(2):126–9 [cited 2025 Aug 3]Available from, http://www.redalyc.org/articulo.oa?id=265531454002. Portuguese.
[57] Balls M. The three rs and the humanity criterion: an abridged version of the principles of humane experimental technique by w.m.s. russell and r.l. burch. nottingham: fund for the replacement of animals in medical experiments (frame); 2009.
[58] Organization for Economic Co-operation and Development. Guidance document on the recognition, assessment and use of clinical signs as human endpoints for experimental animals used in safety evaluation [Internet]. Paris: OECD Publishing; 2002. https://doi.org/10.1787/9789264078376-en. Available from.
[59] Seyed Jafari SM, Shafighi M, Beltraminelli H, Geiser T, Hunger RE, Gazdhar A. Improvement of flap necrosis in a rat random skin flap model by in vivo electroporation-mediated hgf gene transfer. Plast Reconstr Surg 2017;139(5): 1116e–27e.
[60] Seyed Jafari SM, Shafighi M, Beltraminelli H, Weber B, Schmid RA, Geiser T, et al. Efficacy of In Vivo electroporation-mediated il-10 gene delivery on survival of skin flaps. J Membr Biol 2018;251(1):211–9.
[61] Seyed Jafari SM, Blank F, Ramser HE, Woessner AE, Shafighi M, Geiser T, et al. Efficacy of combined in-vivo electroporation-mediated gene transfer of vegf, hgf, and il-10 on skin flap survival, monitored by label-free optical imaging: a feasibility study. Front Surg 2021;8:639661.
[62] Richter GT, Fan CY, Ozgursoy O, McCoy J, Vural E. Effect of vascular endothelial growth factor on skin graft survival in sprague-dawley rats. Arch Otolaryngol Head Neck Surg 2006;132(6):637–41.
[63] Krubaa P, Yogitha PS. Albino Wistar rats: advantages and limitations in biomedical research. SBV J Basic Clin Appl Health Sci 2024;7(2):61–5.
[64] Li J, Yan Y, Chen Y, Fang Q, Hussain MI, Wang LN. Flexible curcumin-loaded Zn-MOF hydrogel for long-term drug release and antibacterial activities. Int J Mol Sci 2023;24(14):11439.
[65] Zhang W, Wang B, Xiang G, Jiang T, Zhao X. Photodynamic alginate Zn-MOF thermosensitive hydrogel for accelerated healing of infected wounds. ACS Appl Mater Interfaces 2023;15(19):22830–42.
[66] Huang K, Liu W, Wei W, Zhao Y, Zhuang P, Wang X, et al. Photothermal hydrogel encapsulating intelligently bacteria-capturing Bio-MOF for infectious wound healing. ACS Nano 2022;16(11):19491–508.
[67] Gwon K, Han I, Lee S, Kim Y, Lee DN. Novel metal–organic framework-based photocrosslinked hydrogel system for efficient antibacterial applications. ACS Appl Mater Interfaces 2020;12(18):20234–42.
[68] Atalay C, Koçkaya EA, Çetin B, Kismet K, Akay MT. Efficacy of topical nitroglycerin and transcutaneous electrical nerve stimulation on survival of random-pattern skin flaps in rats. Scand J Plast Reconstr Surg Hand Surg 2003;37(1):10–3.
[69] Gdalevitch P, Laeken NV, Bahng S, Ho A, Bovill E, Lennox P, et al. Effects of Nitroglycerin ointment on mastectomy flap necrosis in immediate breast reconstruction. Plast Reconstr Surg 2015;135(6):1530–9.
[70] Törkvist L, Löfberg R, Raud J, Thorlacius H. Heparin protects against skin flap necrosis: relationship to neutrophil recruitment and anti-coagulant activity. Inflamm Res 2004;53(1):1–3.
[71] Schein O, Westreich M, Shalom A. Effect of intradermal human recombinant copper-zinc superoxide dismutase on random pattern flaps in rats. Head Neck 2013;35(9):1265–8.
[72] Afrooghe A, Damavandi AR, Ahmadi E, Jafari RM, Dehpour AR. The current state of knowledge on how to improve skin flap survival: a review. J Plast Reconstr Aesthet Surg 2023;82:48–57.
[73] Oluwole O, Fernando WB, Lumanlan J, Ademuyiwa O, Jayasena V. Role of phenolic acid, tannins, stilbenes, lignans and flavonoids in human health – a review. Int J Food Sci Technol 2022;57(10):6326–35.
[74] Serrano J, Puupponen-Pimiä R, Dauer A, Aura AM, Saura-Calixto F. Tannins: current knowledge of food sources, intake, bioavailability and biological effects. Mol Nutr Food Res 2009;53(Suppl 2):S310–29.
[75] Chung KT, Wong TY, Wei CI, Huang YW, Lin Y. Tannins and human health: a review. Crit Rev Food Sci Nutr 1998;38(6):421–64.
[76] Tanwar B, Modgil R. Flavonoids: dietary occurrence and health benefits. Spatula DD 2012;2(1):59–68.
[77 Kim YS, Lee HY, Jang JY, Lee HR, Shin YS, Kim CH. Redox treatment ameliorates diabetes mellitus-induced skin flap necrosis via inhibiting apoptosis and promoting neoangiogenesis. Exp Biol Med (Maywood) 2021;246(6):718–28.
[78] Lu F, Mizuno H, Uysal CA, Cai X, Ogawa R, Hyakusoku H. Improved viability of random pattern skin flaps through the use of adipose-derived stem cells. Plast Reconstr Surg 2008;121(1):50–8.